NATIONAL TRANSPORTATION SAFETY BOARD

Office of Research and Engineering
Washington, DC

Oct 5, 2011

Empire Airlines Flight 8284 Kinematics Extraction Study

Dennis Crider

A. ACCIDENT: CEN09MA142

Location:	Lubbock TX
Date:	January 27, 2009
Time:	Approximately 0437 Central Standard Time
Airplane:	Avions de Transport Régional (ATR) Aerospatiale Alenia ATR 42-320, N902FX

B. GROUP IDENTIFICATION:

No group was formed for this activity.

C. SUMMARY

On January 27, 2009, about 0437 Central Standard Time, an Avions de Transport Régional (ATR) Aerospatiale Alenia ATR 42-320 (ATR 42), N902FX, operating as Empire Airlines flight 8284, was on an instrument approach when it crashed short of the runway at Lubbock Preston Smith International Airport (LBB) in Lubbock, Texas. The captain sustained serious injuries, the first officer sustained minor injuries, and the airplane was substantially damaged. The airplane was registered to Federal Express Corporation (FedEx) and operated by Empire Airlines, Inc., as a 14 *Code of Federal Regulations* (CFR) Part 121 supplemental cargo flight. The flight departed from Fort Worth Alliance Airport (AFW) in Fort Worth, Texas, about 0313. Instrument meteorological conditions (IMC) prevailed, and an instrument flight rules (IFR) flight plan was filed.

D. DETAILS OF INVESTIGATION

Introduction

Aerodynamic degradation due to the presence of airframe ice was investigated using kinematics parameter extraction. The motion of an aircraft in flight is a result of aerodynamic and propulsive forces and moments. To isolate the aerodynamic forces, propulsive forces must be modeled. The ATR-42-320 is equipped with two flat rated 1900 SHP PW-121 turboprop engines. As torque and RPM were recorded by the flight data recorder (FDR), shaft horsepower for each engine could be directly calculated. Net thrust was obtained using these recorded torque and RPM values with the prop efficiency of a similar turboprop. This method neglects exhaust thrust, thus the thrust may be slightly low. A low thrust means that the lift coefficients reported in this study will be slightly high with the overestimation proportional to the sine of angle of attack (the overestimation of lift coefficient increases with angle of attack). As will be seen, this slight overestimation of lift coefficient (C_L) with angle of attack will not affect the conclusions of this report. The drag coefficients (C_D) in this report on the other hand will be low with the underestimation proportional to cosine of angle of attack (the under estimation of drag coefficient decreases with angle of attack).

Several FDR parameters are linear with an intercept/slope form. Experience has shown that installation and other factors can cause the intercept to be offset while the slope remains correct. The following offsets in acceleration data recorded by the FDR were found to match the flight path in the flight path integration described in the performance study.

$\Delta N_z = 0.004963$ g's
$\Delta N_x = -0.00774$ g's
$\Delta N_y = 0.052292$ g's

Drag Coefficient Increment Extraction

It was desired to identify times in the flight where drag coefficient exceeded the level expected with an uncontaminated (no ice degradation) airframe. This was done by subtracting the normal airframe drag coefficient from the drag coefficient required for the recorded aircraft motion. As the aerodynamic model of the ATR 42 was not available at the NTSB, a drag model was extracted using data recorded on the FDR for the accident and a previous flight.

Classically drag coefficient has been modeled as a drag polar. That is a basic airframe drag coefficient plus the induced drag coefficient due to lift. Drag coefficient due to lift has long been known to be proportional to lift coefficient squared (C_L^2). The equation takes the following form.

$$C_D = C_{D\,0\,lift} + (dC_D / dC_L^2)\, C_L^2$$

The terms $C_{D\ 0\ lift}$ and dC_D / dC_L^2 in the above equation can be readily obtained by plotting C_D from the extraction as a function of C_L^2. This is done in Fig 1 for a previous flight and Fig 2 for the accident flight. Since weight was unknown for the previous flight a representative weight was used. Accordingly the C_L will be off linearly which results in the parabolic error in C_L^2 seen above $C_L^2 = 1$. Note that with flaps up, the value of C_L^2 remains less than 1.0 for the accident flight. Accordingly, the slope was taken at values of C_L^2 below 1.

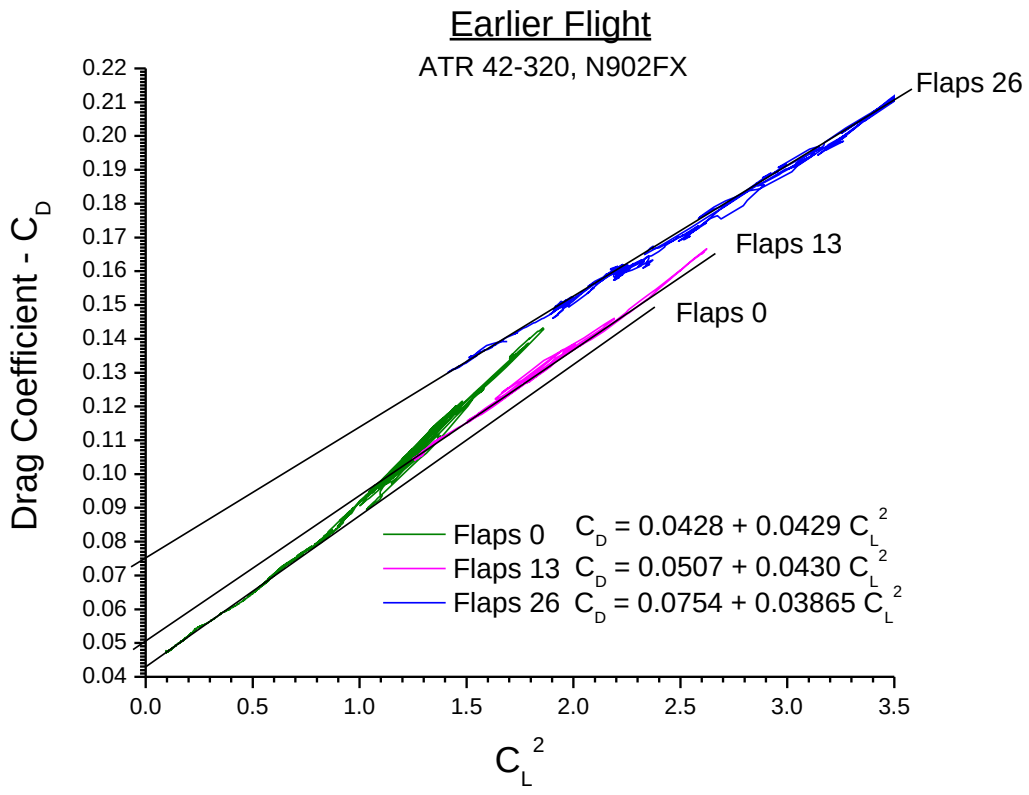

Figure 1 Previous flight drag polar

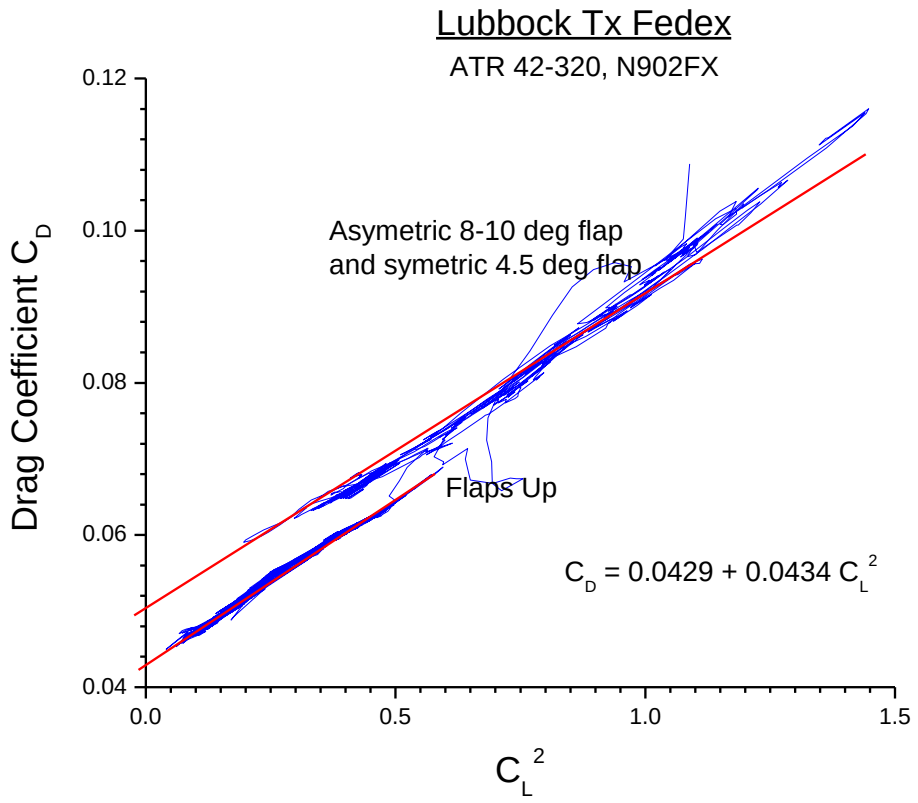

Figure 2 Accident flight drag polar

Thus a drag polar of $C_D = 0.0429 + 0.0434\ C_L^2$ was used to calculate the aircraft's uncontaminated drag coefficients with flaps up.

Interpolating between the flaps up and flaps 13 deg drag polar derived from the previous flight (no ice), the drag polar for 4 ½ degree flaps is estimated to be:

$$C_D = 0.0455 + 0.0429\ C_L^2$$

A flap asymmetry occurred between 4:34:26 and 4:36:02. It was not possible to derive an uncontaminated drag polar for this condition.

The difference between the drag coefficient time history extracted for the accident flight and the drag calculated with the drag polar is given in Fig 3 for the entire flight and in Fig 4 concentrating on the last minutes of flight. This drag increment is not valid during the period of asymmetric flaps.

Figure 3 clearly shows drag increasing beyond the uncontaminated level as the airplane climbed to cruise altitude of 18000 ft about 3:35. The higher drag was maintained until the aircraft descended to 14000 ft at about 4:05 after which time normal drag is seen. As can be seen in Fig

4, by the end of the flap asymmetry, drag has again increased beyond the uncontaminated level and was continuing to increase. It is not possible to determine the beginning of this additional drag since it occurred during the period of asymmetric flaps where the drag increment is invalid.

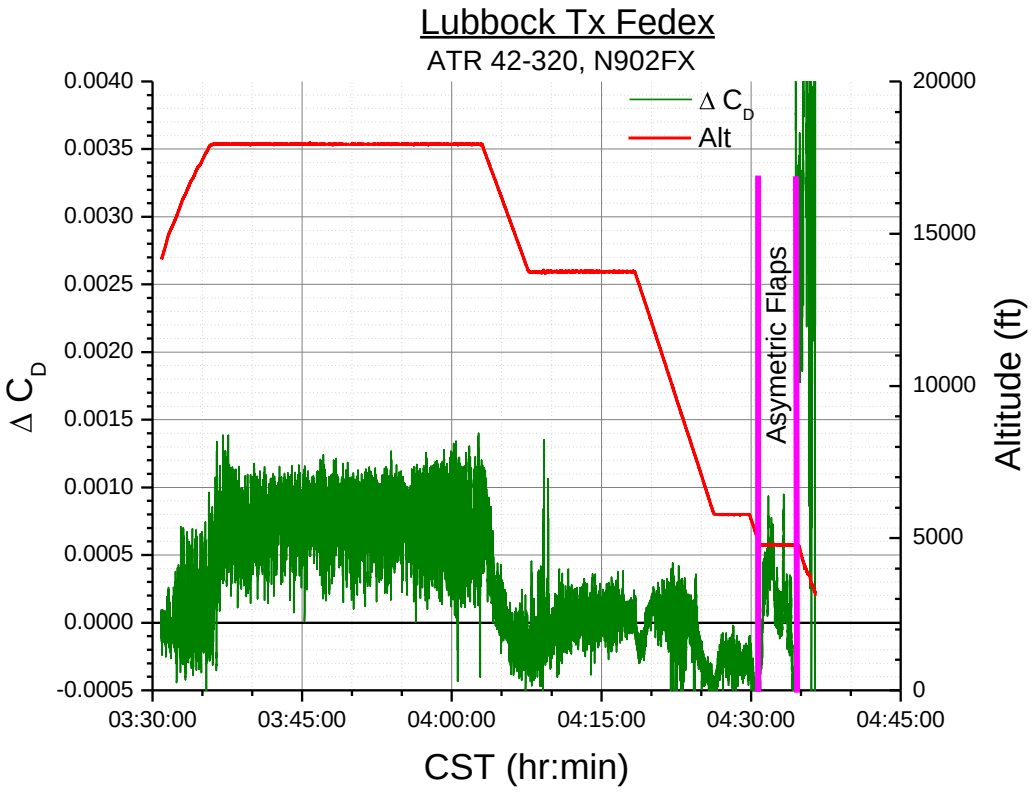

Figure 3 Times with increased drag

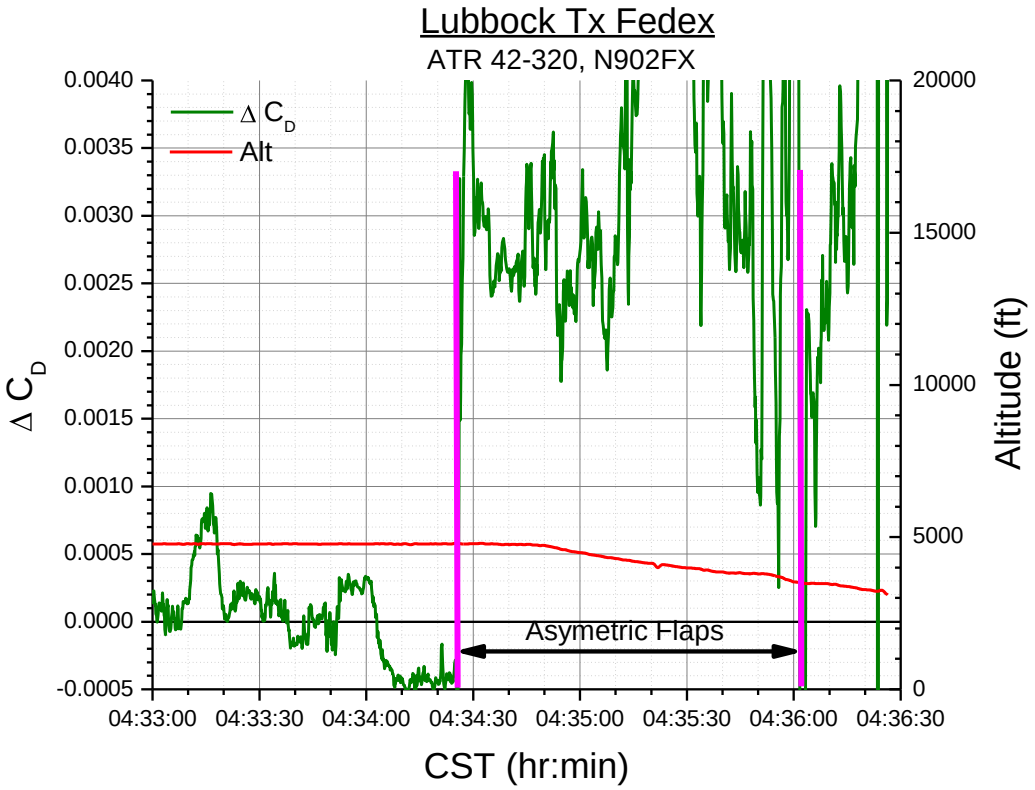

Figure 4 Increased drag before upset

Figure 5 shows a segment of the drag coefficient plotted in Fig 3 on an expanded time scale. The figure shows a high frequency variation in drag that correlates with the recorded load factor which is representative of a level of turbulence. There also appears to be a variation in drag coefficient increment relative to the uncontaminated baseline with a period of between 30 and 60 seconds which may be a reflection of the results of the de-icing boot cycle.

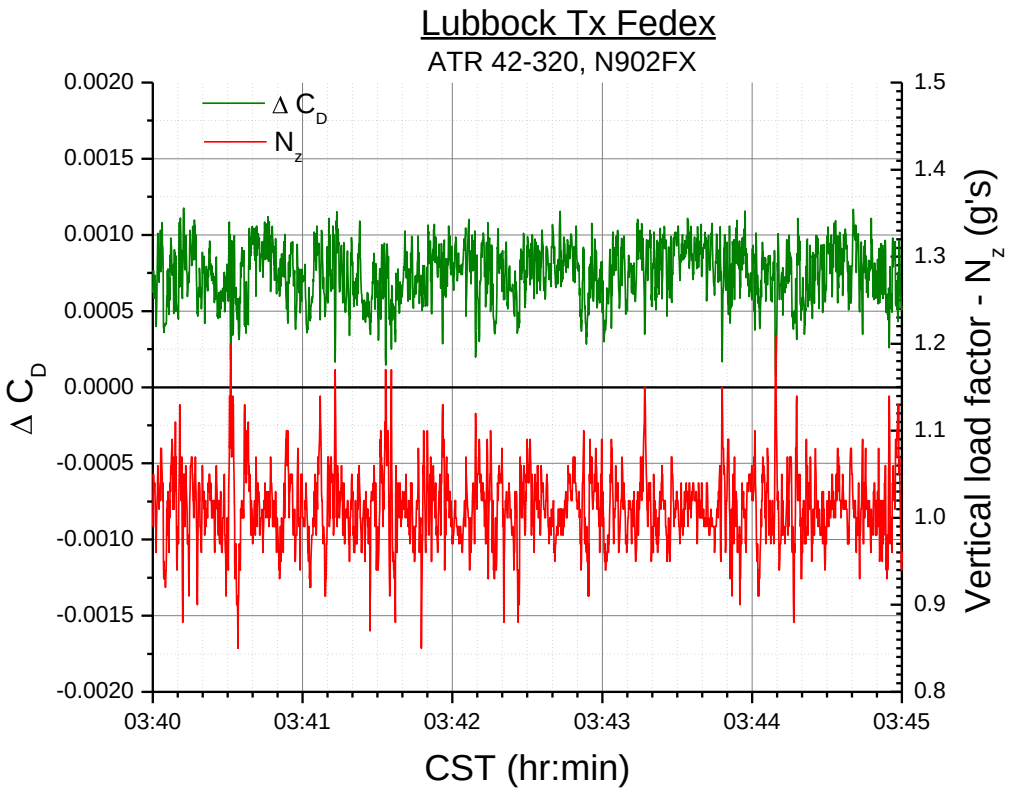

Figure 5 High frequency drag variation

Lift Coefficient Extraction

The aircraft rolled off to the right at about 4:36:21 immediately after stick shaker activation at an angle of attack of about 8 degrees in spite of the prompt application of opposing left wheel (see Fig 6). This behavior was consistent with many accidents and incidents of stall in icing. Accordingly, lift coefficient from the period of the pitch up preceding the roll off to ground impact was cross plotted vs. angle of attack (Fig 7) to produce a 4.5 deg flap lift curve. Figure 7 also shows the lift coefficient from the previous flight which establishes a baseline lift curve. The dashed lines extend the slope of the lift curve to the uncontaminated stall angle of attack above 14 deg. Figure 7 shows the lift coefficient for the accident aircraft increasing approximately linearly with angle of attack until about 8 degrees where a large departure from linear behavior consistent with stall is seen.

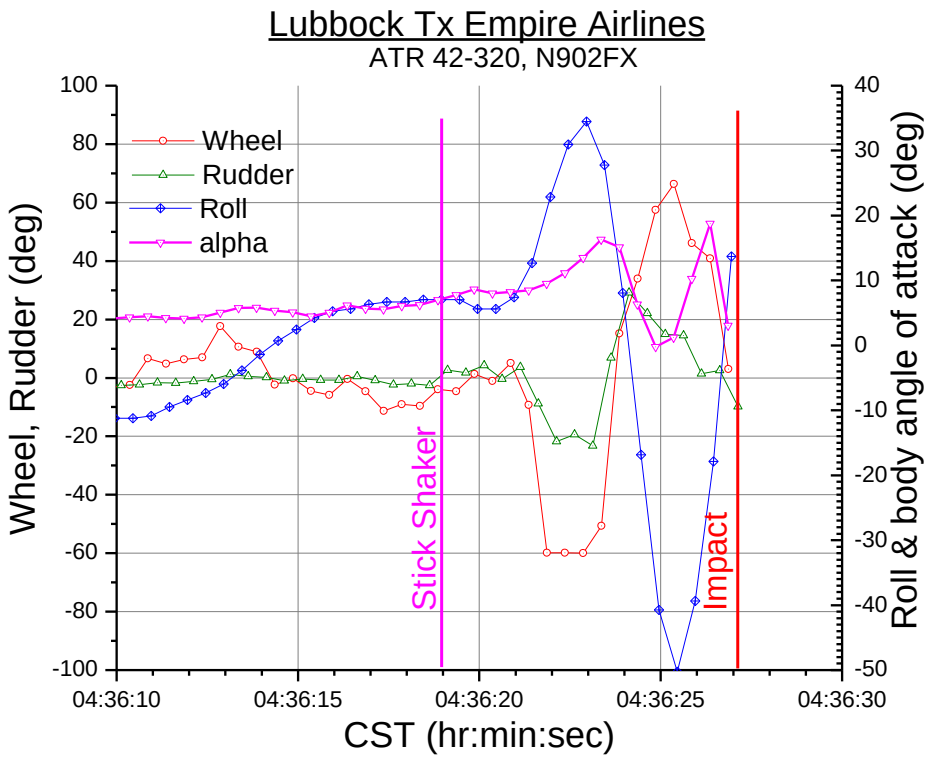

Figure 6 Un-commanded roll

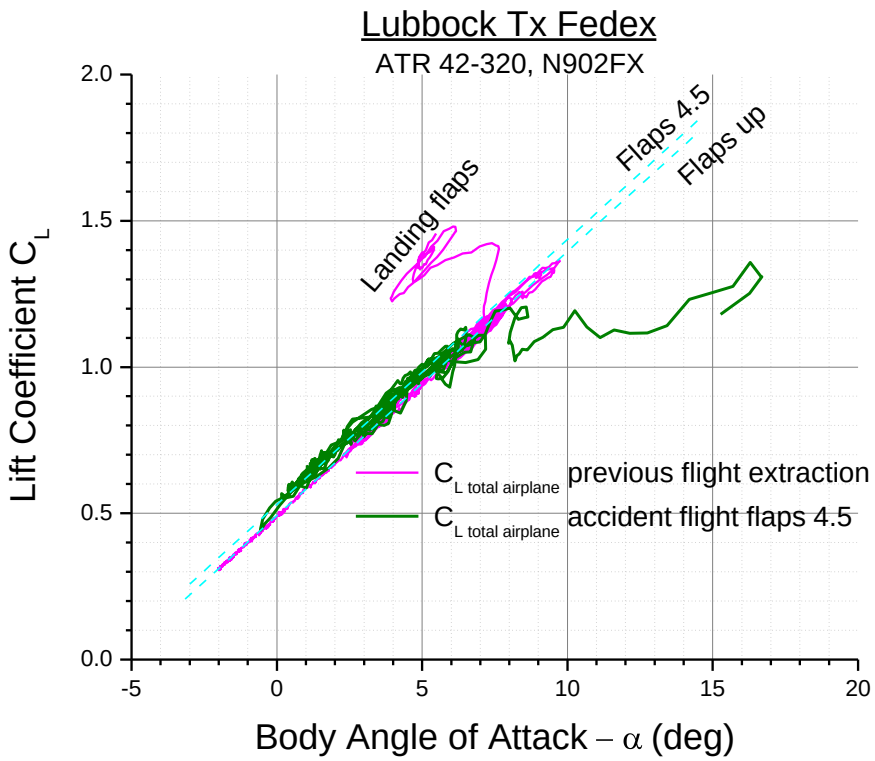

Figure 7 Total airplane lift curve slope

The lift curve extraction for the accident flight shown in Fig 7 has a dip just below 6 deg angle of attack. To explore this anomaly, the period of the 6 deg AOA lift coefficient reduction is plotted on an expanded time scale below (Fig 8) with vertical load factor and angle of attack. The load factors (the major contributor to extracted lift coefficient) for the 6 deg AOA area of reduced lift is circled. Note that the load factor reduction at this point is 4/100 g for 4/10 sec. Note also that the angle of attack is sampled twice a second and would miss any reduction in angle of attack corresponding to the two low load factor points. In comparison, the lift loss at 8 degrees angle of attack covers several seconds.

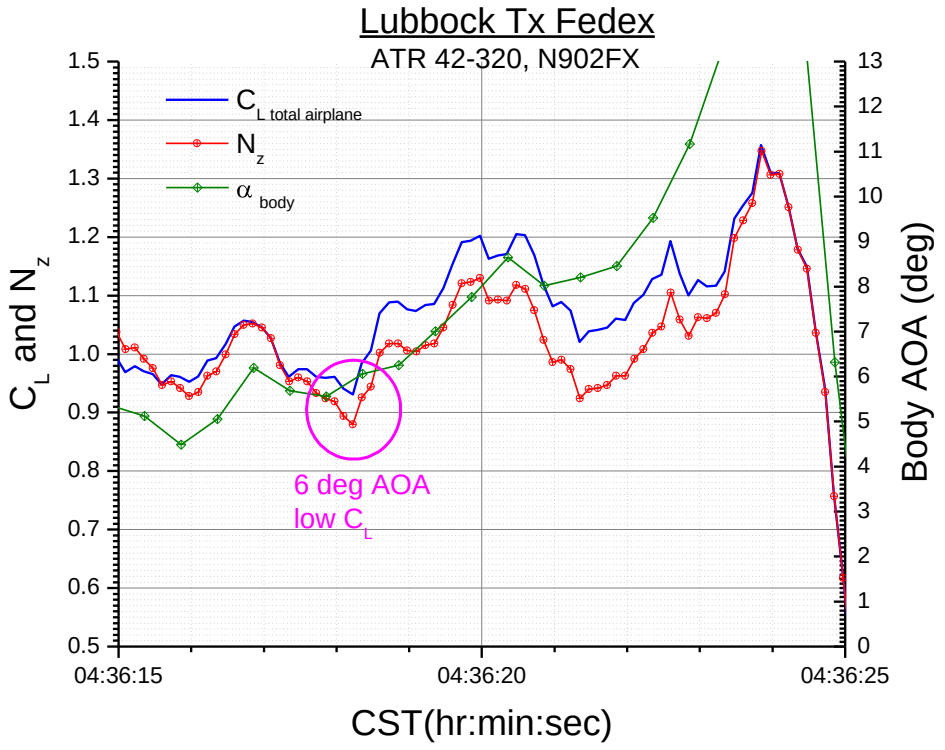

Figure 8 Lift reduction at 6 deg AOA

In response to the un-commanded right roll upset at about 4:36:21, the pilot input left wheel and nose up pitch control. The motion of the airplane is dependent on the total lift coefficient shown in Fig 7 and Fig 8. However, to gain further insight into the wing stall, the effects of these elevator and spoiler inputs were explored.

For pitch control, the FDR recorded left elevator, right elevator and column. Each elevator was recorded twice per second. These elevators were combined to produce an effective four sample per second elevator and the results interpolated to the 8 sample per second common time that will be used to include this elevator in calculations using the extraction output. These parameters are shown in Fig 9.

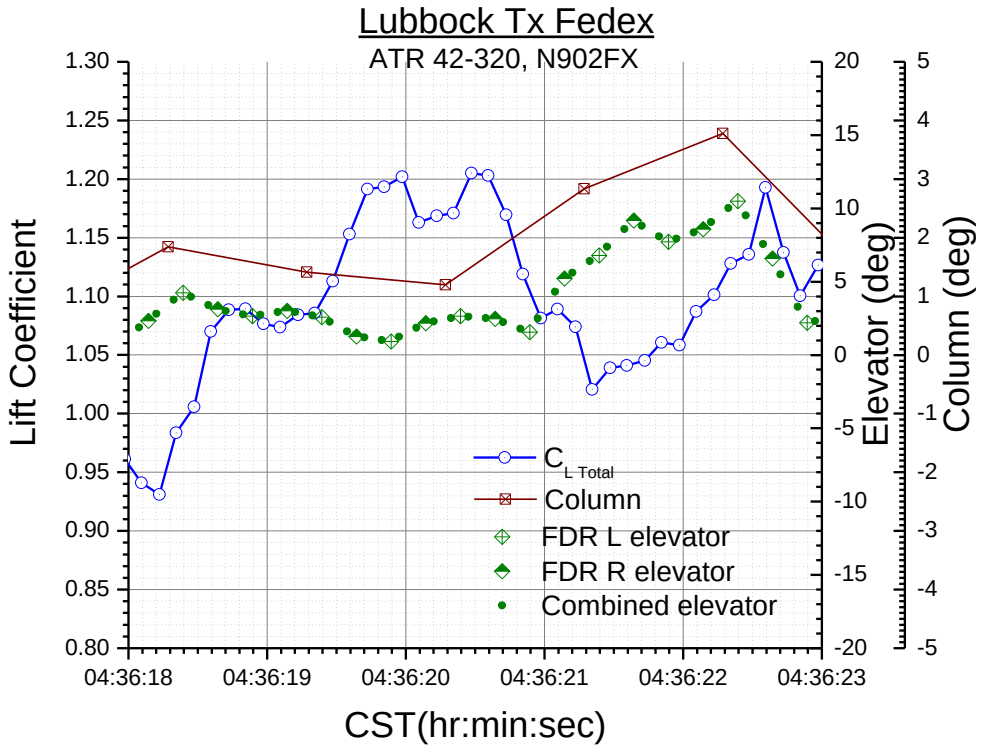

Figure 9 Combined elevator

To determine the time of the roll control input to counter the un-commanded roll as precisely as possible right aileron from the FDR was plotted with FDR left aileron with the sign switched and FDR wheel in Fig 10. Figure 10 also contains a curve labeled "combined aileron" which is the combined right and negative left aileron interpolated to the times of vertical load factor which were used as common break points for the kinematics parameter extraction. Note that in this case we are fortunate in that last zero right aileron position at 4:36:21.4 occurs just before the -9.31 deg wheel sample at 4:36:21.6 fixing the time of the aileron input very precisely.

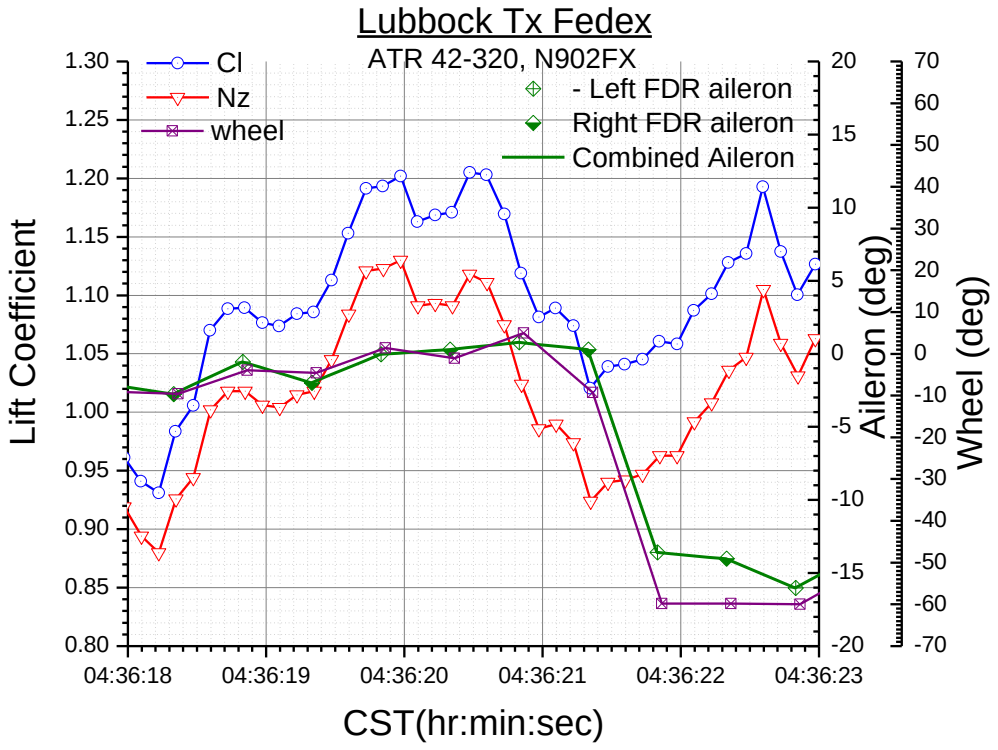

Figure 10 Combined aileron

Elevator effect

The horizontal tail should only be affected by the timing of the stall on the wing through downwash. It should remain well in the linear region such that removing the effect of the elevator with ATR's lift due to elevator coefficient ($C_{L\ \delta e}$) should be a step towards creating a wing body lift coefficient from the extracted total airplane lift. The lift coefficient with the effect of elevator deflection removed ($C_{L\ adj\ elv}$) is shown in Fig 11 as a function of time and plotted as a function of angle of attack in Fig 12.

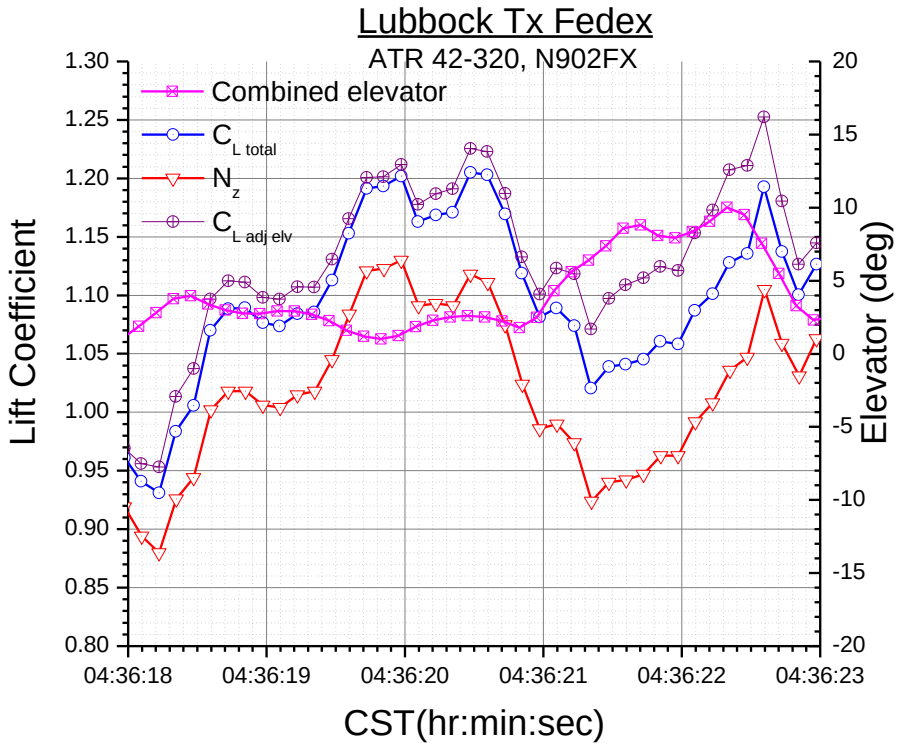

Figure 11 Lift coefficient adjusted for elevator deflection

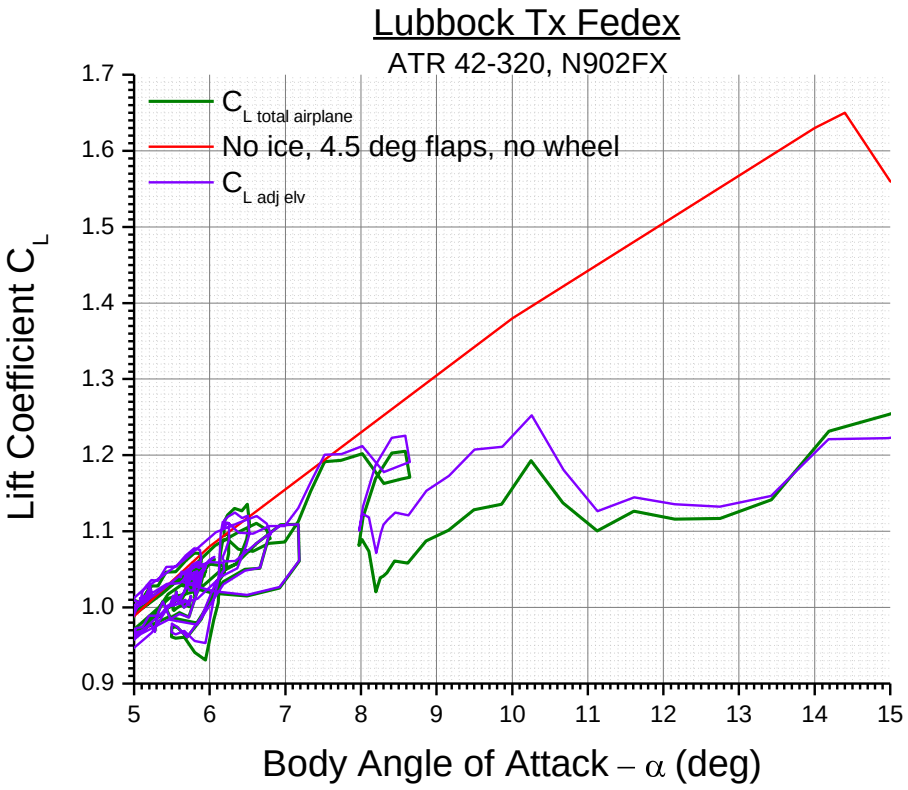

Figure 12 Lift curve adjusted for elevator deflection

Aileron/spoiler effect

Spoiler was derived from the combined FDR aileron deflection (see Fig 10) using the ATR design relationship. This spoiler is shown in Fig 13 together with the lift loss from ATR's aerodynamic model data with this spoiler. The aerodynamic model data is linear and valid for the linear aerodynamic region prior to stall. As can be seen spoilers are deployed just after the minimum in total airplane lift coefficient at 4:36:21.4. If the aircraft were not stalled, the application of this spoiler would result in the decrement in lift as shown in the figure. As can be seen in Fig 13, lift coefficient is increasing during this period and no such lift coefficient decrement is evident with spoiler for the accident flight. At most the data might show a decrease in the rate of lift coefficient increase when the spoilers are deployed. However, the aircraft did respond to the spoiler so some lift loss must exist during this period. This will be addressed in the rolling moment section below.

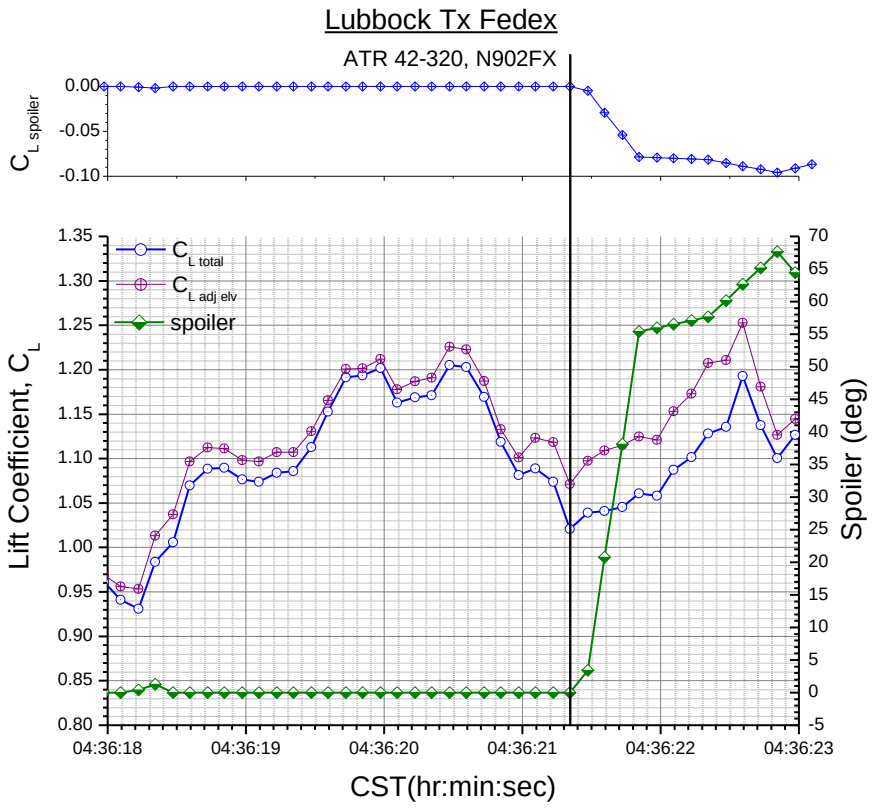

Figure 13 Spoiler lift effect

Pitching Moment Coefficient Extraction at Upset

The total airplane pitching moment coefficient was obtained from the extraction. This was then adjusted for the effect of elevator deflection using ATR's lift due to elevator coefficient ($C_{L\ \delta e}$) and the aircraft geometry (tail length and mean aerodynamic chord) to produce $C_{m\ \text{adjusted for elevator}}$. Pitching moment coefficient is plotted vs. time in Fig 14 and vs. angle of attack in Fig 15. As can be seen in Fig 14, pitching moment becomes dynamic at about 4:36:19.7. A nose down pitching moment developed which the pilot opposed with up elevator to maintain the pitching moment oscillating near zero. As can be seen in Fig 15, pitching moment coefficient shifts nose down at about 8 degrees. This nose down pitching moment is, again, characteristic of a stall.

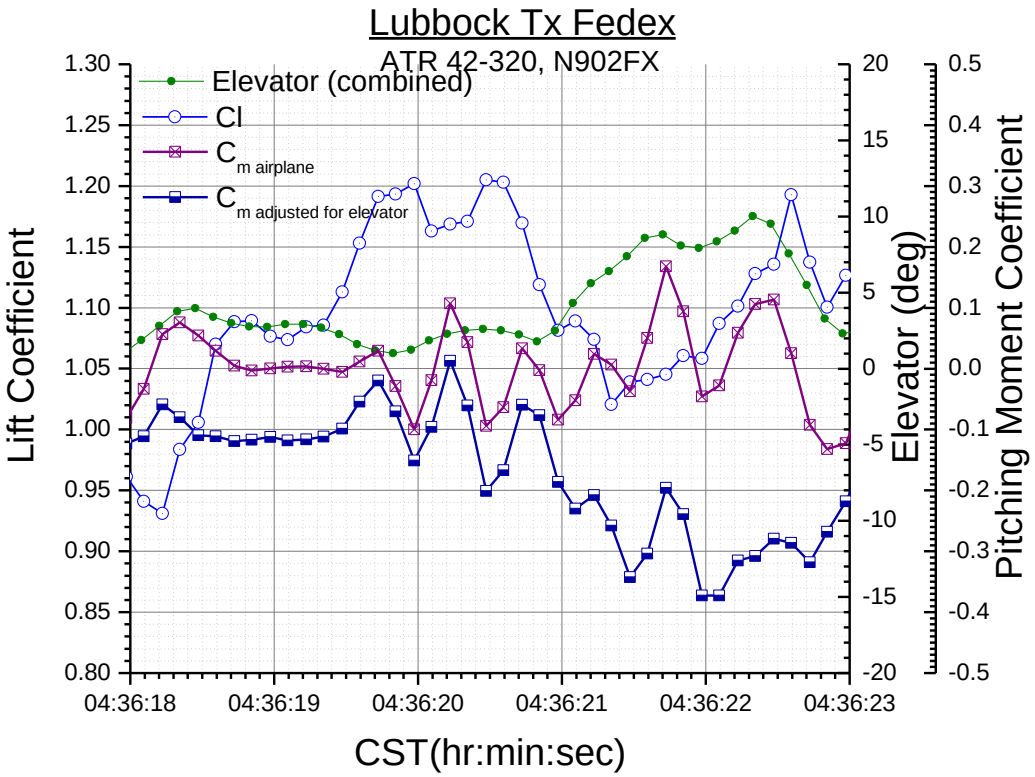

Figure 14 Pitching moment coefficient vs. time

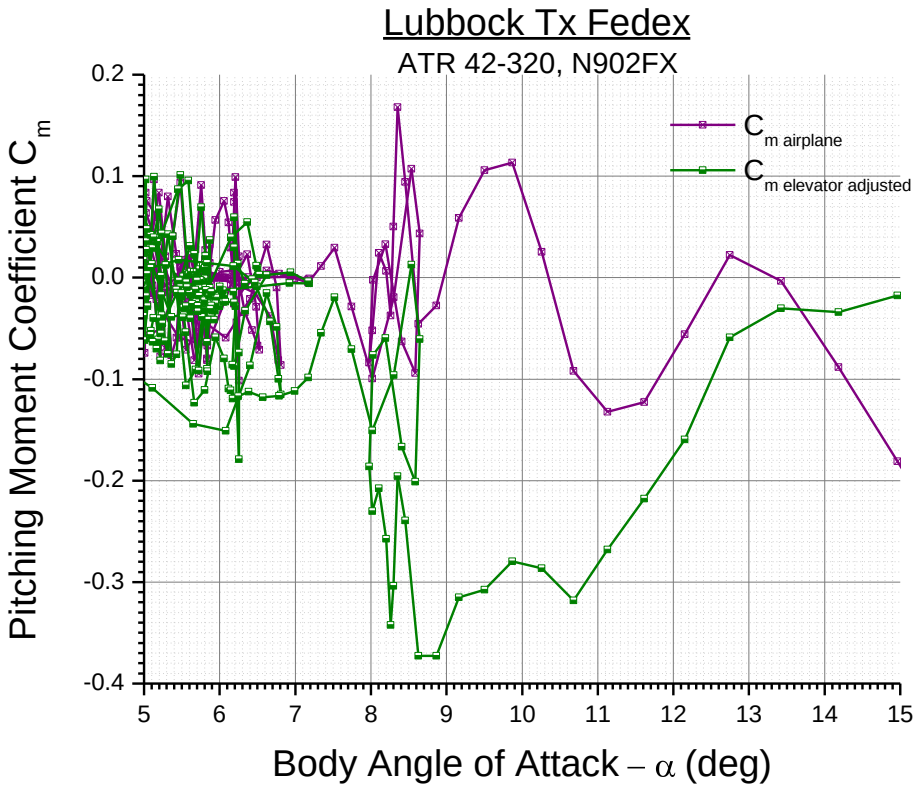

Figure 15 Pitching moment coefficient vs. AOA

Drag Coefficient Extraction at Upset

The difference between the drag extracted for the accident flight around the time of the un-commanded roll and the drag calculated with the 4 ½ deg flap drag polar above is plotted in Fig 16 as a function of time and in Fig 17 as a function of angle of attack. There is a sharp increase in drag just after[1] 4:36:21 and 8 degrees body angle of attack that is consistent with a stall. However, wheel to oppose the roll is input at about this point which would also be expected to increase the drag. Drag coefficient is decreasing between 9 degrees angle of attack to 11 degrees angle of attack. Accordingly, the increase in drag coefficient expected with stall can only be part of the sharp increase in drag just after 8 degrees angle of attack.

[1] Precision in time is limited by the sample rate of the parameters on the FDR (8 Hz for N_z, 4 Hz for N_x and pitch) and is thus less for drag coefficient than for lift coefficient.

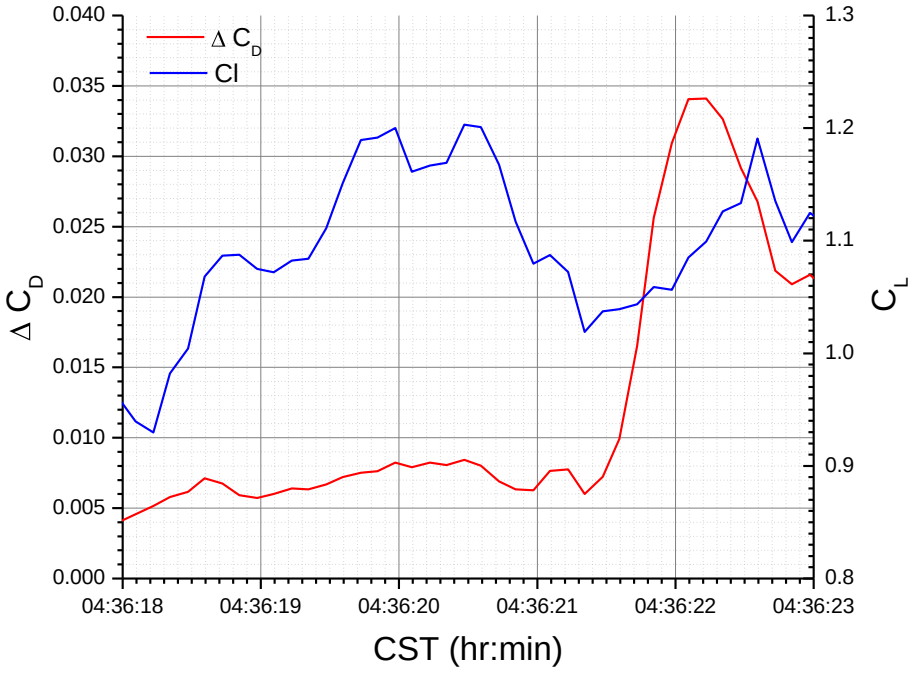

Figure 16 Drag and Total Airplane Lift Coefficient vs. time

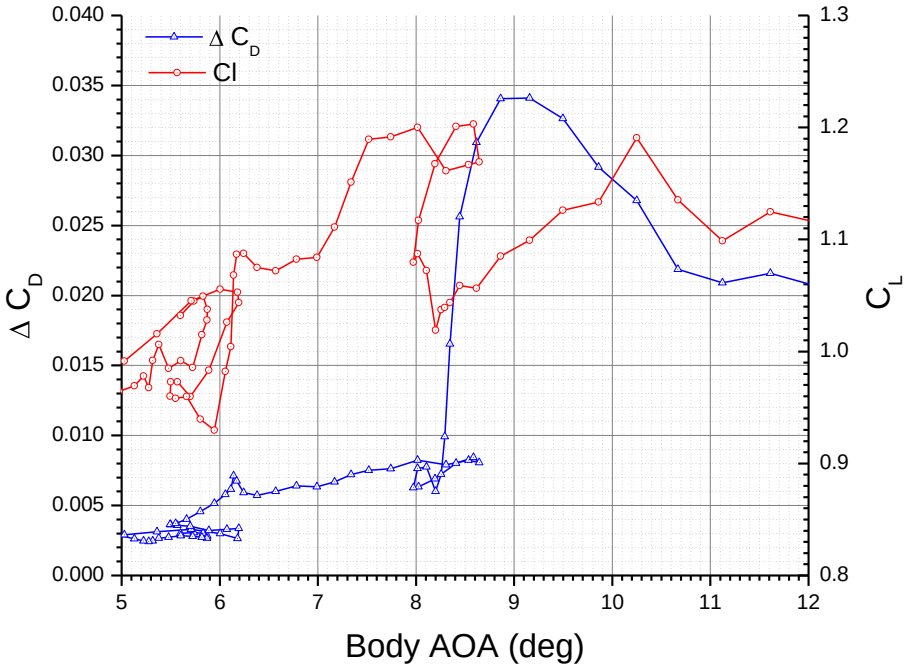

Figure 17 Drag and Total Airplane Lift Coefficient vs. Angle of Attack

Rolling Moment Coefficient Extraction at Upset

The extracted rolling moment coefficient for the accident flight around the time of the un-commanded roll is shown in Fig 18 as a function of time. Rolling moment is plotted vs. angle of attack in Fig 19. Note the discontinuity in rolling moment at 8 degrees angle of attack consistent with asymmetric stall at this point.

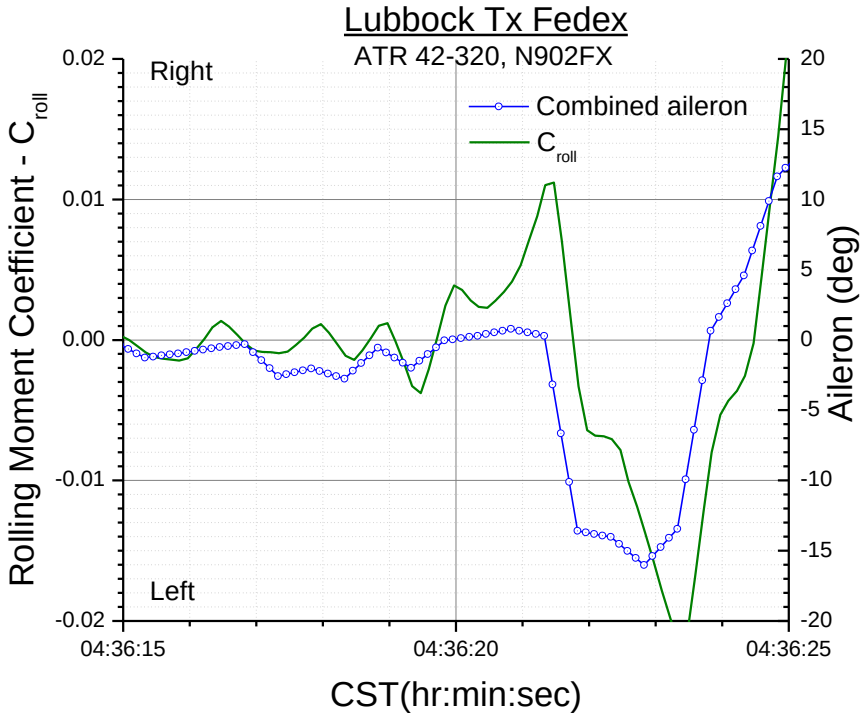

Figure 18 Rolling moment near the upset

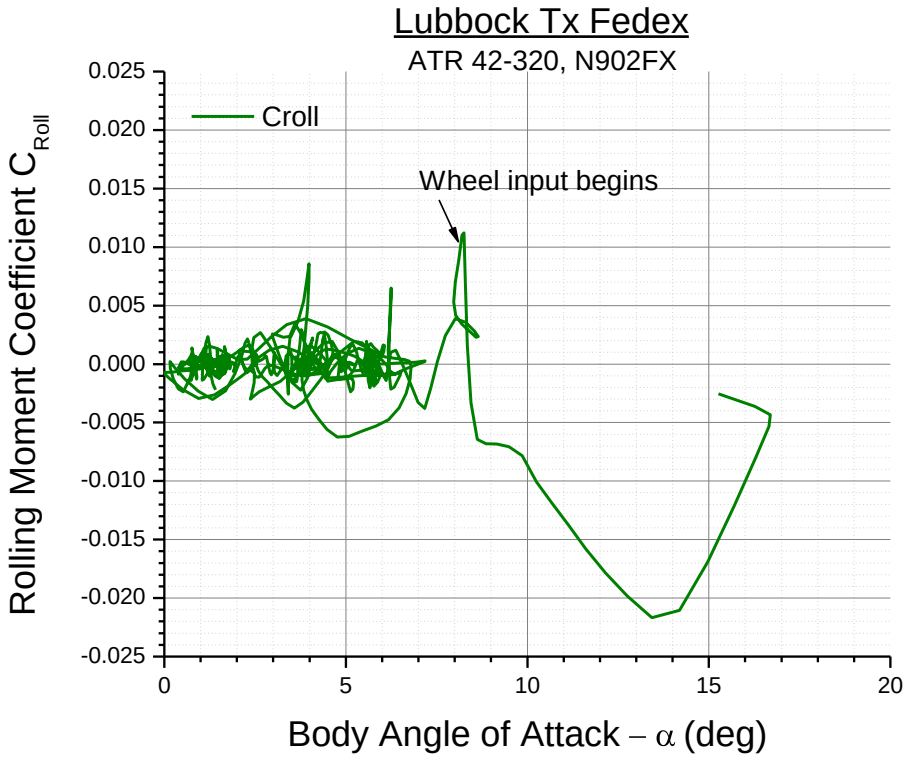

Figure 19 Rolling moment vs. angle of attack

Fig 18 shows a change in rolling moment of approximately -0.0176 over the time period of approximately ½ second when left wheel is applied to counter the un-commanded right roll. Assuming that the asymmetric lift for this rolling moment is centered at the spoiler, the corresponding lift loss for this point in time (4:36:22) is approximately 60% of the un-stalled spoiler effectiveness shown in Fig 13.

The reduced spoiler lift decrement as the spoilers are deflected is evidence that the flow is already separated and the aircraft is in a post stall environment. Further, the lack of lift decrement seen in the total airplane lift coefficient at the time of spoiler deflection is consistent with the ineffective roll control seen in response to the un-commanded roll off.

Yawing Moment Coefficient Extraction at Upset

Extracted yawing moment for the time period of the upset is shown in Fig 20. The delay in yaw response to the rudder is interesting. Note that a right yawing moment increment would be expected with asymmetric stall causing the un-commanded right roll.

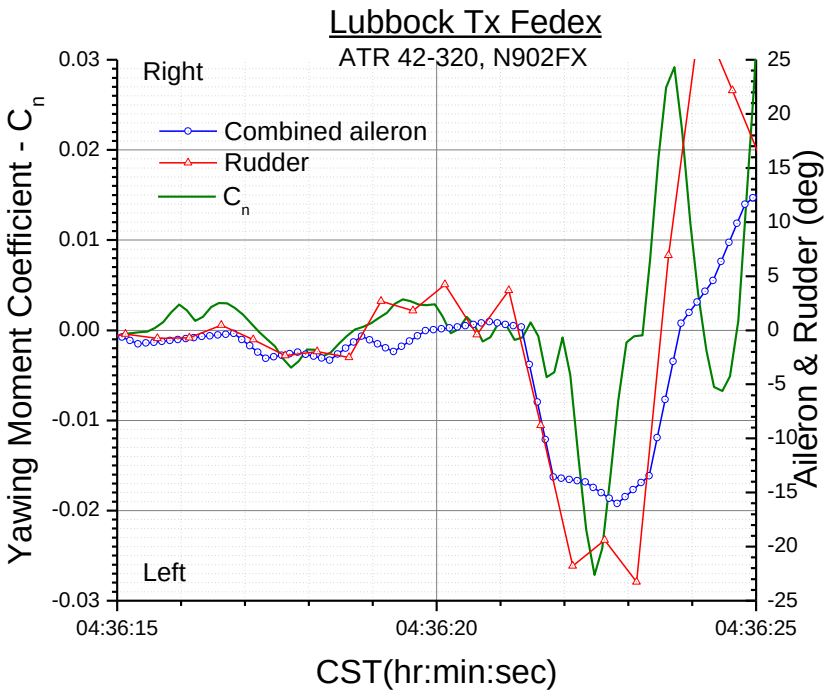

Figure 20 Yawing moment coefficient

Aerodynamic Mechanism for the Upset

The aircraft experienced an un-commanded roll at approximately 8 deg angle of attack which was ineffectively opposed by wheel and rudder. Such an un-commanded roll off coupled with ineffective roll control for recovery is a common characteristic of stall upset accidents and incidents both with and without ice. The un-commanded roll is caused by a rolling moment which requires an asymmetric force at a distance from the centerline of the aircraft. For the history of stall upsets this asymmetric force has been indicative of asymmetric separation (stall) on the wing which in turn produces asymmetric lift and drag that result in the rolling moment.

A spoiler works by inducing an area of separation behind the spoiler which of course produces less lift from the affected area. If, however, the area affected by the spoiler is already separated, as it is in a stall, the decrement in lift due to spoiler will be much less being driven by the force on the spoiler itself deflected above the separated region. ATR added the un-stalled spoiler lift decrement (Fig 13) as an increment to the extracted lift coefficient and interpreted the results as indicating a stall at about 10 degrees angle of attack. This required an alternative explanation for the roll off at 8 degrees angle of attack. ATR suggested an atmospheric rotation due to unknown causes. The performance report showed no evidence of sideslip till rudder was applied after the upset. Thus, such an atmospheric rotation would have to exist without inducing sideslip on the aircraft. Note also that the atmosphere was very stable due to the presence of the inversion that caused the freezing rain. Further, as noted above, the lift loss due to spoiler at the time of initial

deflection was approximately 60% of the pre-stall value. Analytically accounting for a pre-stall spoiler lift decrement that doesn't exist, as ATR has done, unrealistically overestimates the lift coefficient.

Aircraft stall produces a drag increase beyond the drag polar. As Fig 17 shows, a sharp drag increase is evident at about 8 deg angle of attack[2] consistent with a stall. Fig 17 also shows drag decreasing at 10 degrees angle of attack which is inconsistent with the onset of a stall at this angle of attack.

A decrease in downwash angle proportional to the decrease in wing lift will occur at stall. This produces an increase in horizontal tail angle of attack, which results in an upward change in horizontal tail lift and a nose down pitching moment. Figure 15 shows that a nose down pitching moment shift occurs at approximately 8 degrees angle of attack consistent with a stall.

The extracted lift shows a decrease in lift after 4:36:20.5 reaching a minimum shortly after 4:36:21 after which lift coefficient is seen to rise. The corresponding lift curve is almost parallel to the pre-stall slope during this period. As can be seen in Fig 21, torque increased from 30% to 70% during this period with a corresponding increase from 90% to 100% RPM. Such a power increase will lower the angle of attack and increase the flow energy and vorticity on the portion of the wing in the propwash. These effects can allow the portion of the wing in the propwash to remain flying to a higher angle of attack while the portion of the wing outboard of the propwash remains stalled. This is consistent with the lift coefficient during the upset.

[2] Spoiler was also moving at this time so the drag due to spoiler and the drag due to the stall were not separated.

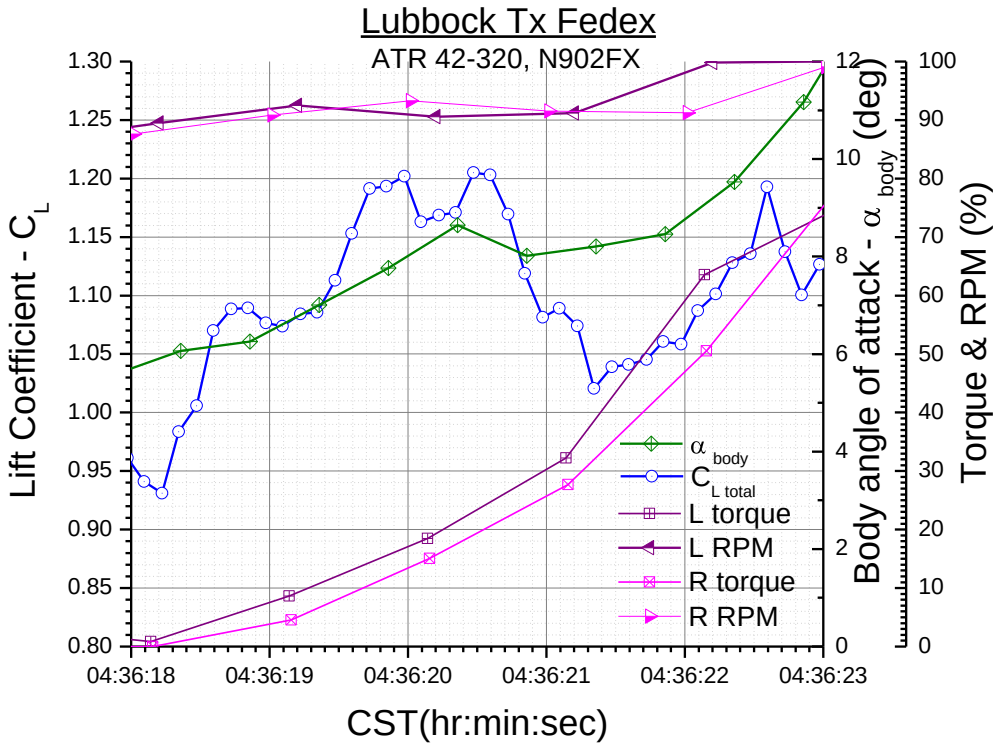

Figure 21 Lift coefficient and power.

Conclusions

A drag level beyond the uncontaminated (no ice) level indicative of an icing encounter occurred from about 3:35 to about 4:05 after which time normal drag is seen. A second greater increase in drag coefficient beyond the no-ice level indicative of a second icing encounter began sometime during the period of asymmetric flaps and continued at least to the upset. The larger drag difference in this period and the rapid onset indicates that this second icing encounter was much worse than the ice handled successfully earlier in the flight.

The aircraft's un-commanded roll off together with the extracted lift, pitch, drag coefficient and rolling moment for the accident shows a stall in icing at approximately 4:36:20 with an angle of attack of approximately 8 degrees about 1 second after the stick shaker activated.